Resolution in Confocal Microscopy

Ann Bui *

PHYS3051 Fields in Physics Project Report

Semester 1 2011

Abstract

We shall investigate resolution within microscopy. The light produce received from a microscope had been approximated with the Debye integral modelling the distribution of light around the focus of a well-corrected lens. From this, computational simulations were performed to investigate the resolution. Resolution specifically regarding (single-photon)confocal and two-photon confocal microscopy was investigated to find that confocal generally has better resolution than the two-photon microscope in both the lateral and optical directions. The resolution of different coloured tags was explored to find that enhanced green fluorescent protein (EGFP) gives greater resolution than red fluorescent (DsRed) protein tag.

Contents

*ann.bui@uqconnect.edu.au,UQ-Australia iGEM Team, University of Queensland, Brisbane, Queensland, Australia

1 Introduction

The specific types of microscopes that we shall investigate are the confocal and two-photon confocal microscopes. With their ability to section into live biologicals, these microscopes play a significant role in science with their role in imaging the interaction between small molecules within cells[1][2][3]. A notable example of this is in the experimental imaging of protein-protein interactions[4]. The identification of these protein-protein interactions is anticipated to 'potentially revolutionise our view of biological and disease pathologies'[5].
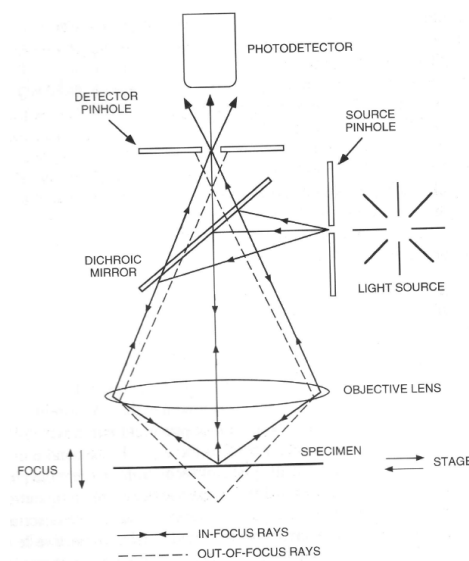

Fig. 2. Light path in a stage scanning LSCM.

Figure 1: Apparatus set up of a confocal microscope[6]. A two-photon confocal microscope would have two light pulses as the light sources whereas a typical confocal microscope would have a single light pulse a the light source. Note that the detector is behind a pinhole, i.e. a small aperture. Only the light focused onto the specimen, i.e. object to be imaged, can be detected through the aperture.

Confocal, with respect to microscopes, refers to the illumination of an object, where in this case, it is confined to a diffraction-limited spot in the object and the detector is similarly confined by an aperture placed at the focus[1], as in Figure 1. This aperture allows for only focused light to reach the detector, this allowing the microscope to perform optical sectioning[7]. This means that the microscope can scan flat 2D section multiple times to create a three-dimensional image of an object.

We shall investigate the physical ability of the confocal and two-photon confocal microscope by calculating its limits under normal operation. Thus, the limitation would be the ability to resolve two points that must pass through a small aperture, at the thus we wish to investigate the behaviour of light around the aperture. Since the light has been focused, we wish to look at the distribution of light near the focus of a lens. Such a light distribution as the one to be derived would not be easily done, if possible, experimentally as we have not considered the inhomogeneities in the object, aberrations, noise and other nonlinearities. We shall assume that the optics is linear such that all light sent to illuminate the object is detected. It would be expected however, that any experimental variations would b=not be that significant compared to the nature of light. The following derivation can be thought of as the best resolution we could ever have if everything worked 'perfectly'.

2   Light at the focus

We wish to find the distribution of light near the focus. Note that confocal microscopy allows for optical section, so our light distribution shall be in the plane of the object as well as in the optical direction. This derivation was motivated by Diaspro[8], supported by Born and Wolf[9].
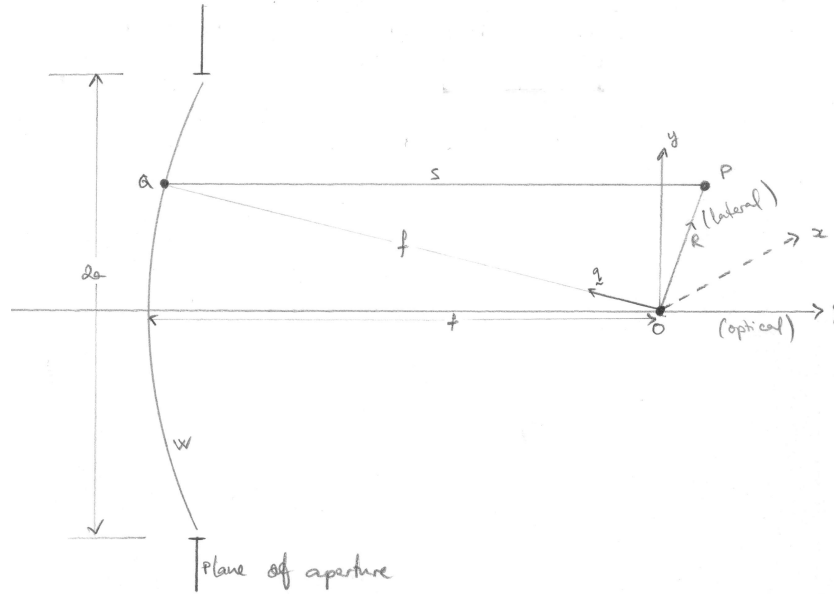

Figure 2: Diagram for derivation[9]. A spherical wavefront at the aperture plane is converging towards the focus at O.

Consider a monochromatic spherical wave at the aperture plane in Figure 2 and converging towards focal point O. Consider a disturbance in the field $U(P)$ at a point P in the neighbourhood of O. Point P is in direction and magnitude of $\mathbf{R}$ from O. We shall assume that $\mathbf{R}$ and a the size of the aperture are small compared to f the radius of the spherical wave that momentarily fills the aperture.

Take point Q to be a point on W the wavefront with $\mathbf{q}$ the unit vector from O to Q. Let the distance between P and Q be s. Define $\frac{A}{f}$ to be the amplitude of the wave at Q. Note that A is arbitrary. We can see that

$$s - f = -\mathbf{q} \cdot \mathbf{R} \implies s = f - \mathbf{q} \cdot \mathbf{R}. \tag{1}$$

From the Huygens-Fresnel Principle[9], we must then have

$$U(P) = -\frac{i}{\lambda} \frac{A \exp\left(-ikf\right)}{f} \iint \frac{\exp\left(iks\right)}{s} dW$$

assuming the variation of W over the wavefront is negligible.

We can see that our wavefront, equivalent to the arc of a sector, is spanned by an angle Ω such that

$$W = f^2 \Omega$$

which implies that a dW a small section of the wavefront is given by

$$dW = f^2 d\Omega \tag{2}$$

where $d\Omega$ is an element of solid angle that dW subtends at O. Hence

$$
\begin{aligned}
U(P) &= -\frac{i}{\lambda}A\frac{\exp(-ikf)}{f}\iint\limits_W \frac{\exp(iks)}{s}dW \\[2mm]
&= -\frac{i}{\lambda}A\frac{\exp(-kf)}{f}\iint\limits_W \frac{\exp(ikf)\cdot\exp(-ik\mathbf{q}\cdot\mathbf{R})}{f-\mathbf{q}\cdot\mathbf{R}}dW \qquad \text{from Eq. 1} \\[2mm]
&= -\frac{i}{\lambda}A\frac{\exp(-ikf)}{f}\iint\limits_W \frac{\exp(ikf)\cdot\exp(-ik\mathbf{q}\cdot\mathbf{R})}{f-\mathbf{q}\cdot\mathbf{R}}f^2 d\Omega \qquad \text{from Eq. 2} \\[2mm]
&= -\frac{i}{\lambda}A\frac{\exp(-ikf)}{f}\iint\limits_W \frac{\exp(ikf)\cdot\exp(-ik\mathbf{q}\cdot\mathbf{R})}{f}f^2 d\Omega \qquad \text{since} \quad f-\mathbf{q}\cdot\mathbf{R}\approx f \\[2mm]
&= -\frac{i}{\lambda}A\frac{\exp(-ikf+ikf)}{f^2}\iint\limits_W \exp(-ik\mathbf{q}\cdot\mathbf{R})\,f^2 d\Omega. \\[2mm]
&= -\frac{i}{\lambda}A\iint\limits_W \exp(-ik\mathbf{q}\cdot\mathbf{R})\,d\Omega \qquad\qquad\qquad\qquad\qquad\qquad (3)
\end{aligned}
$$

Note that this integral runs over all angle Ω where the wavefront W subtends at the focus.

We shall refer to Equation 3 as the Debye integral. We wish to evaluate this integral to calculate the intensity of light near the focus of a lens. So let's define a set of rectangular coordinates centred on O as specified in Figure 2. Define distances r and $a\rho$ such that P is distance r from O and Q is distance $a\rho$ from O. Set coordinates of $P(x,y,z)$ and $Q(\xi,\eta,\zeta)$ such that

$$
\begin{aligned}
x &= r\sin\psi && \xi = a\rho\sin\theta \\
y &= r\cos\psi && \eta = a\rho\cos\theta \\
z &= z
\end{aligned}
$$

where ρ is a factor of Q along plane of aperture.

To find ξ, we know that Q lies on the spherical wavefront W

$$
\begin{aligned}
\implies \xi &= -\sqrt{f^2-a^2\rho^2} \\[2mm]
&= -f\left(1-\frac{a^2\rho^2}{f^2}\right)^{\frac{1}{2}} \approx -f\left(1-\frac{a^2\rho^2}{2f^2}\right)
\end{aligned}
$$

Now, we have $\mathbf{q}=\frac{1}{f}(\xi,\eta,\zeta)$ and $\mathbf{R}=(x,y,z)$, so we can then find

$$
\begin{aligned}
\mathbf{q}\cdot\mathbf{R} &= \frac{1}{f}(\xi x+\eta y+\zeta z) \\[2mm]
&= \frac{1}{f}\left(a\rho\sin\theta\cdot r\sin\psi + a\rho\cos\theta\cdot r\cos\psi - fz\left(1-\frac{a^2\rho^2}{2f^2}\right)\right) \\[2mm]
&= \frac{ar}{f}\rho\cos(\theta-\psi)-z\left(1-\frac{a^2\rho^2}{2f^2}\right). \qquad\qquad\qquad (4)
\end{aligned}
$$

Let's define a set of cylindrical axes about the z-axis. Define dimensionless variables u and v such that u is a unit vector in the z-direction, call this the optical direction and v is a unit vector in the r direction, call this the lateral distance.

$$
u = \frac{2\pi}{\lambda}\left(\frac{a}{f}\right)^2 z \qquad v = \frac{2\pi}{\lambda}\left(\frac{a}{f}\right)r = \frac{2\pi}{\lambda}\frac{a}{f}\sqrt{x^2+y^2}. \qquad\qquad (5)
$$

Note that there is an implicit assumption here. We have assume that we have rotational symmetry, i.e. symmetry about the optical axis.

So we can now express Equation 4 in terms of our new cylindrical coordinates u and v (and angular component).

$$
\begin{aligned}
\mathbf{q} \cdot \mathbf{R} &= \frac{\lambda}{2\pi} \left(\frac{2\pi}{\lambda} \frac{ar}{f} \right) \rho \cos(\theta - \psi) - \frac{\lambda}{2\pi} \left(\frac{2\pi}{\lambda} \frac{a^2}{f^2} z \right) \left(\frac{f^2}{a^2} - \frac{1}{2} \rho^2 \right) \\
&= \frac{\lambda}{2\pi} \cdot v\rho \cos(\theta - \psi) - \frac{\lambda}{2\pi} u \left(\left(\frac{f}{a} \right)^2 - \frac{1}{2} \rho^2 \right) \\
&= \frac{\lambda}{2\pi} \left(v\rho \cos(\theta - \psi) - \left(\frac{f}{a} \right)^2 u + \frac{1}{2} u\rho^2 \right) \\
\implies k\mathbf{q} \cdot \mathbf{R} &= v\rho \cos(\theta - \psi) - \left(\frac{f}{a} \right)^2 u + \frac{1}{2} u\rho^2.
\end{aligned}
\tag{6}
$$

Now, once again, for our wavefront, as is Equation 2, we must have

$$
W = \Omega f^2 \implies dW = f^2 d\Omega. \tag{7}
$$

Looking at the projection of our aperture plane, we wish to change our Cartesian coordinates for W of (ξ, η) to our new cylindrical (well, two dimensions of it) coordinates of (ρ, θ). First, we need to find the Jacobian (not as straightforward as previously).

$$
\begin{aligned}
\text{Jacobian} = \left| \det \begin{pmatrix} \frac{\partial \xi}{\partial \rho} & \frac{\partial \xi}{\partial \theta} \\ \frac{\partial \eta}{\partial \rho} & \frac{\partial \eta}{\partial \theta} \end{pmatrix} \right| &= \left| \det \begin{pmatrix} a \sin\theta & a\rho \cos\theta \\ a \cos\theta & -a\rho \sin\theta \end{pmatrix} \right| \\
&= \left| -a^2 \rho \sin^2 \theta - a^2 \rho \cos^2 \theta \right| \\
&= a^2 \rho \left(\sin^2 \theta + \cos^2 \theta \right) \\
&= a^2 \rho.
\end{aligned}
$$

Then back to Equation 7, we must then have

$$
\begin{aligned}
dW &= a^2 \rho \, d\rho \, d\theta \\
\implies f^2 d\Omega &= a^2 \, d\rho \, d\Omega \\
\implies d\Omega &= \frac{a^2 \, d\rho \, d\theta}{f^2}
\end{aligned}
\tag{8}
$$

So with Equations 6 and 8, the Debye integral characterising the field near the focus, of Equation 3 becomes

$$
U(u, v) = -\frac{i}{\lambda} A \iint\limits_{\Omega} \exp \left(-i \left(v\rho \cos(\theta - \psi) - \left(\frac{f}{a} \right)^2 u + \frac{1}{2} u\rho^2 \right) \right) \frac{a^2 \rho}{f^2} d\rho \, d\theta.
$$

To determine the bounds of integration, note that ρ was a proportion of W and W was across the whole plane. We want our integral to cover the whole lateral plane of our plane of aperture, so we shall take all values of θ. Thus,

$$
\begin{aligned}
U(u, v) &= -\frac{i}{\lambda} \frac{a^2 A}{f^2} \int_0^1 \int_0^{2\pi} \exp \left(-i \left(v\rho \cos(\theta - \psi) - \left(\frac{f}{a} \right)^2 u + \frac{1}{2} u\rho^2 \right) \right) \rho \, d\theta \, d\rho \\
&= -\frac{i}{\lambda} \frac{a^2 A}{f^2} \exp \left(i \left(\frac{f}{a} \right)^2 u \right) \int_0^1 \int_0^{2\pi} \exp \left(-i \left(v\rho \cos(\theta - \psi) + \frac{1}{2} u\rho^2 \right) \right) \rho \, d\theta \, d\rho \\
&= -\frac{i}{\lambda} \frac{a^2 A}{f^2} \exp \left(i \left(\frac{f}{a} \right)^2 u \right) \int_0^1 \int_0^{2\pi} \exp \left(-iv\rho \cos(\theta - \psi) \right) \cdot \exp \left(\frac{1}{2} u\rho^2 \right) \rho \, d\theta \, d\rho
\end{aligned}
$$

Now, this is a foul integral. Note that the integral expression for Bessel functions $J_n(z)$ is[10]

$$\frac{i^{-n}}{2\pi} \int_0^{2\pi} \exp\left(ix\cos\alpha\right) \cdot \exp\left(in\alpha\right) d\alpha = J_n(x).$$

Thus

$$
\begin{aligned}
J_0(x) &= \frac{1^0}{2\pi} \int_0^{2\pi} \exp\left(ix\cos\alpha\right)\exp\left(0\right) d\alpha \\
&= \frac{1}{2\pi} \int_0^{2\pi} \exp\left(ix\cos(\theta-\psi)\right) d(\theta-\psi) \\
&= \frac{1}{2\pi} \int_0^{2\pi} \exp\left(ix\cos(\theta-\psi)\right) d\theta \\
\implies \int_0^{2\pi} \exp\left(-v\rho\cos(\theta-\psi)\right) d\theta &= 2\pi J_0(v\rho).
\end{aligned}
$$

So back to Equation 9, we have

$$
\begin{aligned}
U(u,v) &= -\frac{i}{\lambda}\frac{a^2 A}{f^2} \exp\left(i\left(\frac{f}{a}\right)^2 u\right) \int_0^1 2\pi J_0(v\rho) \exp\left(-\frac{1}{2}iu\rho^2\right) \rho d\rho \\
&= -\frac{2\pi i a^2 A}{\lambda f^2} \exp\left(i\left(\frac{f}{a}\right)^2 u\right) \int_0^1 J_0(v\rho) \exp\left(-\frac{1}{2}iu\rho^2\right) \rho d\rho
\end{aligned}
\tag{9}
$$

So Equation 9 gives us the distribution of the field at Point P of a monochromatic spherical wave near the focus of a lens. This can represent the focusing of light from a laser onto an object to be imaged with a confocal microscope.

However, we do not observe the amplitude of a field. Instead, we observe the intensity, which is the mod square of the amplitude. We can define a value to give us this intensity, call this value the point source function. Define the point source function to be

$$\text{point source function} = |U(u,v)|^2 = U(u,v)^\dagger U(u,v). \tag{10}$$

Our point source function gives us the distribution of light in the optical and lateral dimensions. In an experimental biology sense, this would represent the absorption pattern of a uniform fluorophore solution in the neighbourhood of the focus, in the space domain.

Now, for the confocal microscope, we have pointwise illumination and detection, so both the illumination and detection of photons are at the focus of a lens. So we can model the distribution of light intensity around the point of illumination and detection with our point source functions for illumination and detection respectively.

We can think of the (normalised) point source function as a probability function. Each point has a probability of being illuminated and, independently, every illuminated point has a chance of being detected. So we can define our point source function for the image from a confocal microscope as the product of these point source function as in Equation 11

$$\left|U_{\text{confocal}}\right|^2 = \left|U_{\text{det}}\right|^2 \left|U_{\text{ill}}\right|^2 \tag{11}$$

For the two-photon confocal microscope, we still have pointwise illumination and detection. Each photon for illumination and detection still obeys the point source function. However, we now have

illumination from two photon, who then combine to give off the one photon for detection. So the image from a two-photon microscope is proportional to the product of the probability of two photons independently illuminating the object and the probability that a photo is detected. Thus we have the point source function for a two-photon confocal microscope defined as in Equation 12.

$$|U_{\text{2-photon}}|^2 = \left(|U_{\text{det}}|^2\right)^2 |U_{\text{ill}}|^2 \tag{12}$$

3   Simulations

We now have an expression for the intensity of light at the focus of a lens. We wish to see how this behaves in a physically realistic situation. We shall plot the intensity patterns of light for varying wavelengths to produce the final image. These simulations were performed with MATLAB, see section A.

We shall test the resolution for different wavelengths. Biologicals are usually tagged with more than one colour, which allows the observer to see more than one object[11]. This would be particularly useful for looking at more than one entity, such as protein-protein interactions where we wish to see two separate proteins within the one specimen.

We have chosen two fluorescent tags that are commonly used in labs, enhanced green fluorescent protein (EGFP) and (DsRed). These have the corresponding wavelengths as in Table 1. For confocal microscopy, we have a laser illuminating our object. Light from the object is then detected. Note that the illumination and detection wavelengths are different.

Table 1: Wavelengths corresponding to protein tags[11]

Protein	Illumination$_{\text{Confocal}}$ (nm)	Illumination$_{\text{2-photon}}$ (nm)	Detection (nm)
EGFP	488	900	520
DsRed	568	1064	645

Confocal imaging with EGFP is shown in Figure 3. Note that the plot is proportional to the intensity or probability of the light imaged. The confocal microscope image with EGFP is produced from the illumination of the object at 488 nm, Figure 3a, then detection at 520 nm 3b. The observed image is taken to be the product of the illuminated and detected distributions as given in Figure 3c.

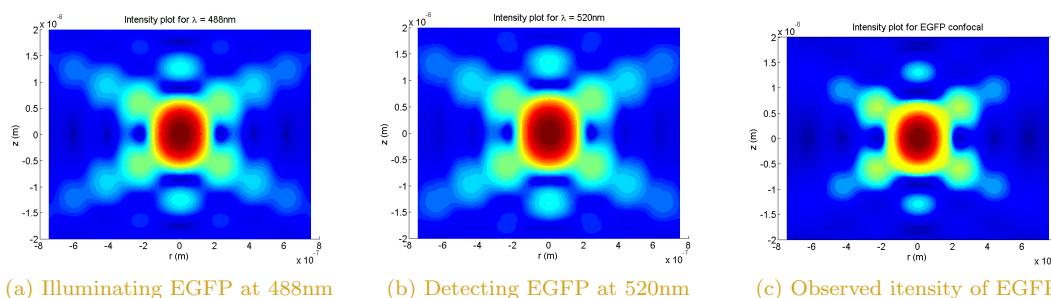(a) Illuminating EGFP at 488nm   (b) Detecting EGFP at 520nm   (c) Observed itensity of EGFP

Figure 3: Intensity distributions for confocal microscope for enhanced green fluorescent protein (EGFP). Red indicates highest intensity with blue the lowest intensity.

Confocal imaging with DsRed is shown in Figure 4. The confocal microscope image with DsRed is produced from the illumination of the object at 568 nm, Figure 4a, then detection at 645 nm 4b. The observed image is taken to be the product of the illuminated and detected distributions as given in Figure 4c.

Two-photon confocal imaging with EGFP is shown in Figure 5. The two-photon confocal microscope image with EGFP is produced from the illumination of the object at 900 nm, Figure 5a, then detection at

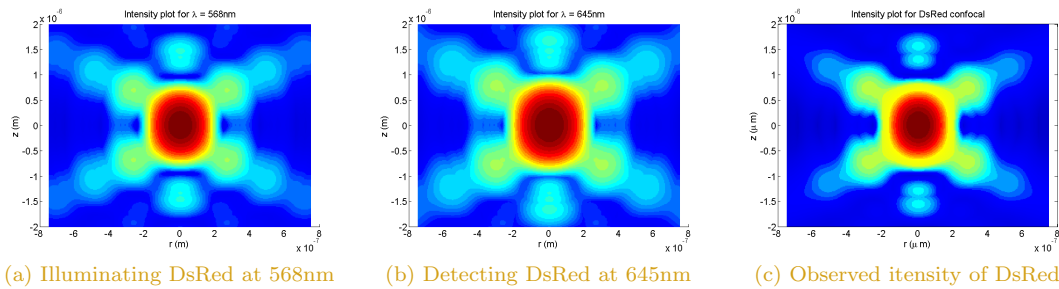(a) Illuminating DsRed at 568nm   (b) Detecting DsRed at 645nm   (c) Observed itensity of DsRed

Figure 4: Intensity distributions for confocal microscope for DsRed. Red indicates highest intensity with blue the lowest intensity.

520 nm 5b. The observed image is taken to be the product of the illuminated and detected distributions as given in Figure 5c.

(a) Illuminating EGFP at 900nm   (b) Detecting EGFP at 520nm   (c) Observed itensity of EGFP
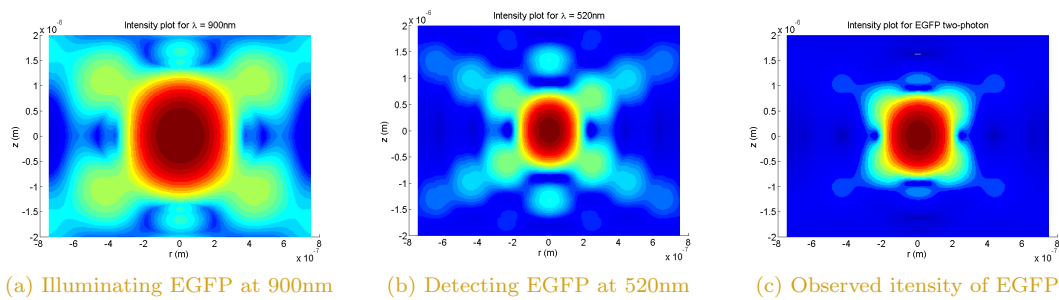
Figure 5: Intensity distributions for two-photon confocal microscope for enhanced green fluorescent protein (EGFP). Red indicates highest intensity with blue the lowest intensity.

Two-photon confocal imaging with DsRed is shown in Figure 6. The two-photon confocal microscope image with EGFP is produced from the illumination of the object at 1064 nm, Figure 6a, then detection at 645 nm 6b. The observed image is taken to be the product of the illuminated and detected distributions as given in Figure 6c.

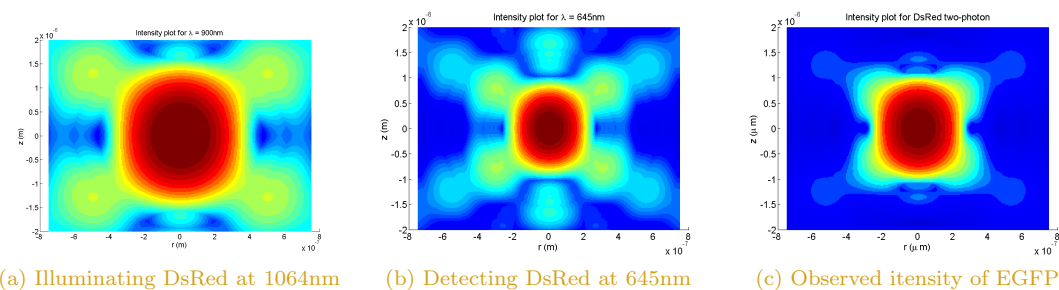(a) Illuminating DsRed at 1064nm   (b) Detecting DsRed at 645nm   (c) Observed itensity of EGFP

Figure 6: Intensity distributions for two-photon confocal microscope for DsRed. Red indicates highest intensity with blue the lowest intensity.

Note that the plots are symmetric about the $r = 0$ axis, as we would expect as we have assumed this. This means that on the plane of the image, we expect to see a somewhat circular pattern. Note also that there are nonzero intensities above and below $z = 0$. This implies that we can look below the surface of the object. This would be practical if we were to look at a function inside a cell, without opening the cell.

8

4 Resolution

For the purposes of comparing resolution in this report, we shall consider the full-width half-maximum (FWHM) value. As this sounds, this is the width of the peak at half of its maximum value. So for all observed lights, we shall calculate the FWHM value with MATLAB, Section A, with results recorded in Table 2.

There is speculation that confocal microscopes can focus to smaller than optical wavelengths[12][13]. This would be justified from our simulations, provided that it was performed very well experimentally. Note that we have assumed independence, otherwise referred to as incoherence, in our handling of the point source functions of light. Our light source is a monochromatic laser, so we would expect some coherence. This the interaction of the phase of the light could be included in further calculations. Note that it would be unlike for light, illuminated with detected, to be completely coherent, so we would expect partially coherent light. This could also result in a different handing of resolution[14][15][16].

Table 2: Full-width half-maximum of observed intensities

Protein	Lateral (μm)	Optical (μm)
Confocal EGFP	0.18	0.11
Two-photon EGFP	0.21	0.12
Confocal DsRed	0.22	0.13
Two-photon DsRed	0.25	0.15

Note that we have found that confocal microscopes give greater resolution compared to the two-photon microscope, yet two-photon microscopy is still common[17]. Note that the illuminating light is of greater (almost twice the) wavelength of the single-photon confocal microscope. This means that the object, usually a live biological sample, would have light of lower energy illuminating it, thus reducing the issue of killing the sample with the light [2][18], yet still retain the optical section ability characteristic of confocal microscopy.

We can see that in general the confocal microscope has a smaller FWHM value,which indicates that each spot from the confocal is smaller than that of the two-photon confocal microscope in both the optical and lateral directions. This implies that the confocal can image an object to greater lateral resolution, but also to greater depth resolution than a two-photon confocal microscope.

The FWHM value is only one method of measuring resolution. Another common method is the Rayleigh criteria [19] where we would consider the distance between the first diffraction minimum and the central maximum as being the resolution of the optical signal.

Note that although there FWHM might be in the order of hundreds of nanometres, there are methods, based on biological experience, to further infer information from images. Due to the pointlike collection of images, the confocal microscope is a scanning microscope. This means that there must a time-lag between the collection of each point. When looking at two small objects simultaneously, methods such as fluorescence correlation spectroscopy[20][21] take advantage of this by looking at the location of two entities over time to judge the interaction or just the biological localisation nature of proteins. Note that there is a distinction between localisation and resolution in physics, however this is not relevant in this discussion, but could be explored in a more rigorous exploration.

Despite an improvement in resolution, two-photon microscopes are still used in laboratories. We need to further our investigation into other aspects of microscopy before a decision to favour a particular microscope is used, even when comparing single and two-photon confocal microscopes. There may be some preferences in using light with a longer wavelength due to the biologicals being imaged, thus preferences for a two-photon microscope, however there are further physical reasons to favour the two-photon microscope, despite its lack of resolution.

The obvious improvement is that a two-photon microscope would have an improvement in with the amount of noise in a measurement. This could be shown by considering a Gaussian beam of light. For longer wavelengths of light, we would expect smaller divergence of light over its travelled path compared

to shorter wavelengths of light. Since the two-photon and confocal microscopes are scanning, there would be less light form neighbouring scans with the longer wavelength, thus we would wish to use light of the longer wavelength. Thus, the two-photon microscope would be favoured.

Note also that this analysis has really just been simulations performed on an established model of light at a focus. This does not include any inhomogeneities in the lens material or media in which the imaging has been performed. Note also that confocal and two-photon microscopes are complex systems and involve more than just light being focused at a point then received at some other focus. A more rigorous analysis could consider the specific optics of the microscope and the differences in the media being imaged.

5   Conclusion

We find that a confocal microscope has greater resolution than a two-photon microscope. The depth resolution is greater than the lateral resolution for both green and red protein tags. The enhanced green fluorescent protein tag has greater resolution than the DsRed protein tag.

References

[1] W. B. Amos and J. G. White. How the confocal laser scanning microscope entered biological research. *Biology of the Cell*, 95(6):335–42, 2003.

[2] Fritjof Helmchen and Winfried Denk. Deep tissue two-photon microscopy. *Nature Methods*, 2(12): 932–40, 2005.

[3] J G White, W B Amos, and M Fordham. An evaluation of confocal versus conventional imaging of biological structures by fluorescence light microscopy. *The Journal of Cell Biology*, 105(1):41–48, 1987.

[4] Won-Ki Huh, James V. Falvo, Luke C. Gerke, Adam S. Carroll, Russell W. Howson, Jonathan S. Weissman, and Erin K. O'Shea. Global analysis of protein localization in budding yeast. *Nature*, 425(6959):686–91, 2003.

[5] Albert-László Barabási and Zoltán N. Oltvai. Network biology: understanding the cell's functional organization. *Nature Reviews Genetics*, 5:101–13, Februray 2004.

[6] Stephen W. Paddock. *Confocal Microscopy Methods and Protocols*. Human Press Inc., 1999.

[7] G.J. Brakenhoff, P. Blom, and P Barends. Confocal scanning microscopy with high-aperture lenses. *Journal of Microscopy*, 117:219–32, 1979.

[8] James Jonkman and Ernst Stelzer. *Confocal and Two-Photon Microscopy: Foundations, Applications, and Advances*, chapter 5, pages 101–26. Wiley-Liss, Inc, 2002.

[9] Max Born and Emil Wolf. *Principles of Optics*, chapter 8, pages 412–516. Cambridge University Press, seventh edition edition, 1999.

[10] G.B. Arfken and H.J. Weber. *Mathematical Methods for Physicists*. Harcourt Academic Press, sixth edition, 2001.

[11] Stefan Jakobs, Vinod Subramaniam, Andreas Schönle, Thomas M. Jovin, and Stefan W. Hell. EGFP and DsRed expressing cultures of Escherichia coli imaged by confocal, two-photon and fluorescence lifetime microscopy. *FEBS Letters*, 479(3):131–35, 2000.

[12] M. Schrader and S. W. Hell. Potential of confocal microscopes to resolve in the 50 to 100 nm range. *Applied Physics Letters*, 69(24):3644–6, 1996.

[13] W. Lukosz. Optical systems with resolving powers exceeding the classical limit. *Journal of the Optical Society of America*, 56(11):1463–72, 1966.

[14] D. Grimes and B. Thompson. Two-point resolution with partially coherent light. *Journal of the Optical Society of America*, 57(11):1330–4, 1967.

[15] B. P. Ramsay, E. L. Cleveland, and O. T. Koppius. Criteria and the intensity-epoch slope. *Journal of the Optical Society of America*, 31(1):26–33, 1941.

[16] J. L. Harris. Diffraction and resolving power. *Journal of the Optical Society of America*, 54(7): 931–6, 1964.

[17] Victoria E. Centonze and John G. White. Multiphoton excitation provides optical sections from deeper within scattering specimens than confocal imaging. *Biophysical journal*, 75(4):2015–24, 1998. http://linkinghub.elsevier.com/retrieve/pii/S000634959877643X.

[18] G. H. Patterson and D. W. Piston. Photobleaching in two-photon excitation microscopy. *Biophysical Journal*, 78(4):2159–62, 2000.

[19] A. J. den Dekker and A. van den Bos. Resolution: a survey. *Journal of the Optical Society of America A*, 14(3):547–57, 1997.

[20] Elliot L. Elson and Douglas Magde. Fluorescence correlation spectroscopy. i. conceptual basis and theory. *Biopolymers*, 13(1):1–27, 1974.

[21] Douglas Magde, Elliot L. Elson, and Watt W. Webb. Fluorescence correlation spectroscopy. ii. an experimental realization. *Biopolymers*, 13(1):29–61, 1974.

A MATLAB Code

A.1 Single wavelength intensity distributions

This was the code used to calculate the values of the intensities for each wavelength of light. This also generated the figures for the single wavelengths.

```matlab
%% Fields report
% To generate all figures for report
% The main variable will be the wavelength lambda

% As we vary lambda, we can see the intensity plots around the focus
% The focus will be at position (0,0)

% From the plots we should be able to determine the resolution!
clear

%% variables

lambda = 488e-9; % nm
NA = 1.3; % (a/f) in written notes

%% Hard coded relations

% 0.0008 and 0.0003 give 5001 steps
% 0.0133 and 0.005 give 301 steps
z = -2:0.0133:2; % nm
z = z*1e-6;
r = -0.75:0.005:0.75; % nm
r = r*1e-6;

% p = 0:0.0002:1;
% vp = v.*p;
% expup = -0.5*1i*u.*p.*p;

coeff = -1i*2*pi*(1.3^2)/(1.518*lambda);

%% Integrating


Intensity = zeros(length(r)); % j by k
j = 1; % row counter
while j <= length(r), % moving down row, v fixed u varied
    u = (2*pi/lambda) * (1.3^2) * z(j) * (1/1.518);
    k = 1; % column counter
    while k <= length(z), % moving through columns of one row, u fixed v varied
        v = (2*pi*1.3/lambda)  * r(k);
        integrand = @(p)besselj(0,v*p) .* exp(-0.5*1i*u*(p.*p)) .* p;
        Amplitude = coeff*exp(-1i* ((1.518/1.3)^2) * u) * quadgk(integrand,0,1);
        Intensity(j,k) = abs(Amplitude).^2;
%        Intensity(j,k) = 1;
        k = k+1;
    end
    clc
    progress = j/length(r) % Yes, I'm impatient
```

```
    j = j+1;
end

figure(1)
surface(r,z,Intensity, 'EdgeColor','none')
view([0 90])
xlabel('r (\mu m)')
ylabel('z (\mu m)')
zlabel('Intensity')
title('Intensity plot for \lambda = ')
```

A.2 Combining the single wavelength intensity distributions

This took the dataset formed from the result of all of the individual wavelength distribution calculations.

```
%% Fields Project handling plots

clear
load('allwavelengths.mat')

%% Normalising

u = (2*pi/1064e-9) * (1.3^2) * z * (1/1.518);
v = (2*pi*1.3/1064e-9)  * r;
Intensity1064 = Intensity1064/sqrt( trapz(u,trapz(v,Intensity1064))^2);

u = (2*pi/900e-9) * (1.3^2) * z * (1/1.518);
v = (2*pi*1.3/900e-9)  * r;
Intensity900 = Intensity900/sqrt( trapz(u,trapz(v,Intensity900))^2);

u = (2*pi/645e-9) * (1.3^2) * z * (1/1.518);
v = (2*pi*1.3/645e-9)  * r;
Intensity645 = Intensity645/sqrt( trapz(u,trapz(v,Intensity645))^2);

u = (2*pi/520e-9) * (1.3^2) * z * (1/1.518);
v = (2*pi*1.3/520e-9)  * r;
Intensity520 = Intensity520/sqrt( trapz(u,trapz(v,Intensity520))^2);


u = (2*pi/568e-9) * (1.3^2) * z * (1/1.518);
v = (2*pi*1.3/568e-9)  * r;
Intensity568 = Intensity568/sqrt( trapz(u,trapz(v,Intensity568))^2);

u = (2*pi/488e-9) * (1.3^2) * z * (1/1.518);
v = (2*pi*1.3/488e-9)  * r;
% for j = 1:length(v),
%     Intensity488(j,:) = (4*Intensity488(j,:).* (v.^2));
% end
Intensity488 = Intensity488/sqrt( trapz(u,trapz(v,Intensity488))^2);


% Intensity488 = Intensity488*1e-10;
% Intensity568 = Intensity568*1e-10;
```

```
% Intensity520 = Intensity520*1e-10;
% Intensity645 = Intensity645*1e-10;
% Intensity900 = Intensity900*1e-10;
% Intensity1064 = Intensity1064*1e-10;



%% Combine the intenisities


TwophotonRed   = log(Intensity1064.^2 .* Intensity645);
TwophotonGreen = log(Intensity900.^2 .* Intensity520);

ConfocalRed   = log(Intensity568.* Intensity645);
ConfocalGreen = log(Intensity488 .* Intensity520);



%% figures
% figure(2)
% surface(r,z,TwophotonRed, 'EdgeColor','none')
% view([0 90])
% xlabel('r (\mu m)')
% ylabel('z (\mu m)')
% zlabel('Intensity')
% title('Intensity plot for DsRed two-photon')
%
% figure(2)
% surface(r,z,TwophotonGreen, 'EdgeColor','none')
% view([0 90])
% xlabel('r (\mu m)')
% ylabel('z (\mu m)')
% zlabel('Intensity')
% title('Intensity plot for EGFP two-photon')
%
%
%
% figure(5)
% surface(r,z,ConfocalRed, 'EdgeColor','none')
% view([0 90])
% xlabel('r (\mu m)')
% ylabel('z (\mu m)')
% zlabel('Intensity')
% title('Intensity plot for DsRed confocal')

% figure(5)
% surface(r,z,ConfocalGreen, 'EdgeColor','none')
% view([0 90])
% xlabel('r (\mu m)')
% ylabel('z (\mu m)')
% zlabel('Intensity')
% title('Intensity plot for EGFP confocal')


%% Finding FWHM
```

```matlab
[TRFWHMI TRFWHMJ] = find(TwophotonRed >= log(0.5*exp(max(max(TwophotonRed)))));

TRFWHMI = abs(151*ones(size(TRFWHMI)) - TRFWHMI);

TRFWHMJ = abs(151*ones(size(TRFWHMJ)) - TRFWHMJ);


TRFWHMr = z(151+max(TRFWHMJ))
TRFWHMz = r(151+max(TRFWHMI))




[TGFWHMI TGFWHMJ] = find(TwophotonGreen >= log(0.5*exp(max(max(TwophotonGreen)))));

TGFWHMI = abs(151*ones(size(TGFWHMI)) - TGFWHMI);

TGFWHMJ = abs(151*ones(size(TGFWHMJ)) - TGFWHMJ);

TGFWHMr = z(151+max(TGFWHMJ))
TGFWHMz = r(151+max(TGFWHMI))




[CRFWHMI CRFWHMJ] = find(ConfocalRed >= log(0.5*exp(max(max(ConfocalRed)))));

CRFWHMI = abs(151*ones(size(CRFWHMI)) - CRFWHMI);

CRFWHMJ = abs(151*ones(size(CRFWHMJ)) - CRFWHMJ);

CRFWHMr = z(151+max(CRFWHMJ))
CRFWHMz = r(151+max(CRFWHMI))




[CGFWHMI CGFWHMJ] = find(ConfocalGreen >= log(0.5*exp(max(max(ConfocalGreen)))));

CGFWHMI = abs(151*ones(size(CGFWHMI)) - CGFWHMI);

CGFWHMJ = abs(151*ones(size(CGFWHMJ)) - CGFWHMJ);

CGFWHMr = z(151+max(CGFWHMJ))
CGFWHMz = r(151+max(CGFWHMI))
```